

0017-9310(95)00159-X

An experimental study of boiling on a wicked surface

M. P. MUGHAL and O. A. PLUMB†

Department of Mechanical and Materials Engineering, Washington State University, Pullman, WA 99164-2920, U.S.A.

(Received 10 June 1994 and in final form 12 April 1995)

Abstract—An open horizontal heat pipe consisting of a condenser, an adiabatic section, and an evaporator is used to study boiling of R-11 on a surface covered with a porous wick. Porous metal wicks having two different thicknesses and with and without channels cut in their surfaces are examined. For these types of surfaces the heat flux increases very dramatically with increases in excess temperature once boiling is initiated. At an excess temperature of a few degrees Kelvin this rapid increase in heat flux stops and a more gradual increase is observed. It is postulated that this represents a transition from what is termed nucleate boiling where the evaporator surface beneath the wick is exposed primarily to liquid and film boiling which results when a vapor film blankets the surface. The experimental results illustrate that the performance of the evaporator can be improved significantly by cutting channels in the porous wick. In this study the heat flux at which the transition from what is termed nucleate boiling to film boiling was increased by 200% by cutting channels in the evaporator wick.

INTRODUCTION

The transfer of heat utilizing heat pipes has been of considerable research interest during the past twenty years because of the numerous applications. These include waste heat utilization [1], solar energy [2], thermal energy storage systems [3], cooling of micro-electronic components [4] and spacecraft applications [5]. The heat pipe has been traditionally studied as a system [6] in which case the various design and operating parameters including the working fluid have been varied in order to optimize performance for a particular application. Many studies have focused on the various operating limits [1] and how these might be extended.

The performance of a heat pipe can be limited by the performance of a number of the components including the condenser, the wick and the evaporator. In this paper we report the results of an experimental study aimed at improving the performance of these components. The evaporator in particular is emphasized, however, some consideration of the wick and the condenser must be included since the three are inextricably linked in a functioning heat pipe. A porous metal wick, similar to those commonly used in practice, is considered. Such wicks offer a number of advantages in that they can be designed to move the necessary flux of liquid from condenser to evaporator and are known to deliver relatively high fluxes at low temperature difference both in the condensation and boiling modes of operation.

Shekarriz and Plumb [7] have demonstrated that an

interrupted porous surface can offer enhanced performance compared to a plane surface during condensation. Thus, it may be possible to improve heat pipe performance, in cases where the performance is limited by the condenser, by using an interrupted porous surface as opposed to a solid porous surface. In addition, there exist some indications [8] and intuitive arguments that boiling heat transfer on a porous surface can be enhanced using an interrupted porous surface. The porous wick complicates the boiling process in that it provides additional sites for nucleation and modifies the movement of the liquid and vapor to and from the heated surface in addition to changing the effective thermal conductivity near the surface. Previous studies [1] have led to the conclusion that at low heat flux heat transfer is primarily by conduction through the flooded wick. At higher values of the heat flux nucleation first occurs on the solid surface and later in the wick. Moss and Kelley [9] reported results of experiments with water on a planar evaporator coated with a stainless steel wick 1/4 in thick. In order to explain their results they proposed two models. In the first, it was assumed that the vaporization occurs at the liquid–vapor interface. In the second, a vapor blanked was assumed to develop at the base of the wick. In this model the liquid vaporized at the edge of the vapor-filled layer near the heated surface. The vapor finds its way out of the wick by flowing along the surface and escaping through the larger pores. As the heat flux is increased one would expect that the vapor will experience increased difficulty in leaving the surface resulting in a thicker vapor layer and the potential for either a higher temperature difference or a lower heat flux. This leads to the postulate that an

† Author to whom correspondence should be addressed.

NOMENCLATURE

A	area [m ²]	w	width of wick [m].
h_{fg}	heat of vaporization [kJ kg ⁻¹]	Greek symbols	
K	permeability [m ²]	δ	liquid film thickness on condenser [m]
K_r	relative permeability	μ	dynamic viscosity [kg m ⁻¹ s ⁻¹]
k_{eff}	effective thermal conductivity [W m ⁻¹ K ⁻¹]	ρ	density [kg m ⁻³]
L_e	effective wicking length [m]	σ	surface tension [N m ⁻¹]
\dot{m}_1	evaporation-condensation rate [kg s ⁻¹]	ϕ	contact angle.
P	pressure [N m ⁻²]	Subscripts	
P_c	capillary pressure [N m ⁻²]	c	refers to condenser
q	heat flux [W m ⁻²]	e	refers to evaporator
Q	total heat transfer [W]	l	a liquid phase property
r	effective pore radius [m]	sat	saturation condition
T	temperature [K]	w	refers to wick.
ΔT_{sub}	degree of subcooling at condenser [K]		

interrupted porous surface might enhance performance.

The objective of the work to be reported was to study through experimentation the performance of several wick geometries on a horizontal heat pipe. The focus is on the evaporator, however, some discussion of the wick and the condenser is included. The horizontal geometry was selected since the porous wick is most commonly applied in situations where the use of gravitational forces to move liquid from the condenser to the evaporator is not convenient.

In what follows the experimental set up is first discussed. A model for predicting the wicking limit for the experimental heat pipe is then presented. This model is useful in interpreting the experimental data since interpretation depends on whether the heat pipe is condenser limited, evaporator limited, or wick limited. In the next section the results will be discussed

and finally the summary and conclusions are presented.

EXPERIMENTAL APPARATUS

The experimental heat pipe is a rectangular horizontal surface 203 mm long \times 76 mm wide as shown in Fig. 1. This surface is made up of an evaporator section, an adiabatic section, and a condenser section. The condenser and evaporator sections are 76 mm \times 63.5 mm and the adiabatic section is 76 mm \times 76 mm. The entire surface can be covered with a sheet of porous material which can provide the wicking action to move liquid from the condenser to the evaporator. At the evaporator, immediately beneath the wick, is a copper plate in which several thermocouples are embedded. Thermocouple locations are indicated in Fig. 1. A thin film heat flux meter (RDF Corp.,

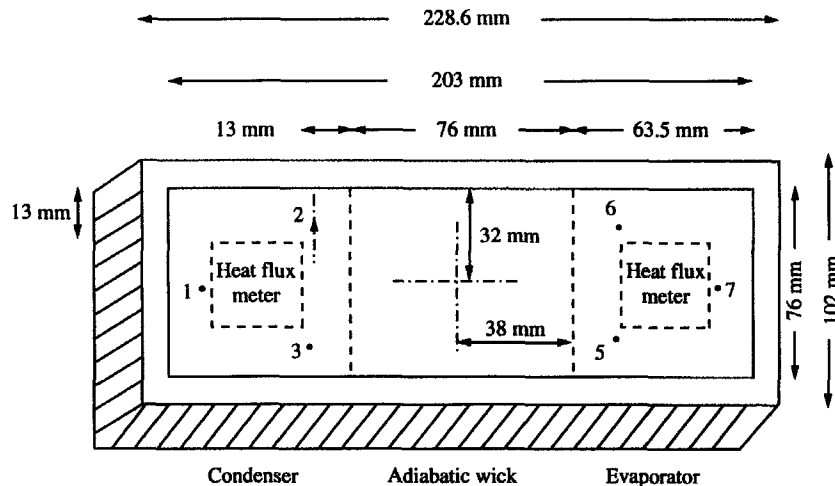


Fig. 1. Schematic of experimental heat pipe.

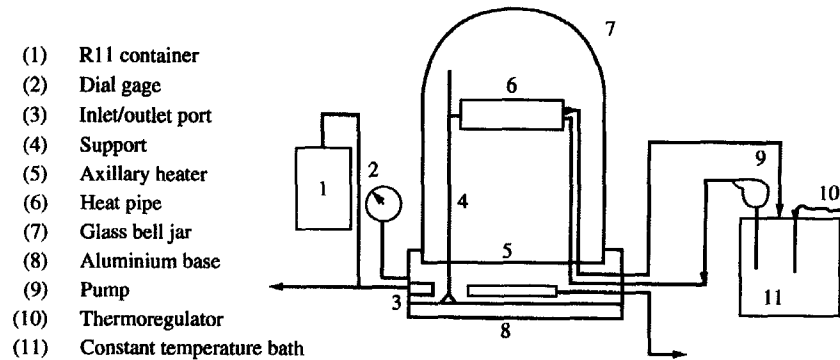


Fig. 2. Schematic of the experimental system.

Hudson, NH) is sandwiched between the copper plate and a heating element that is constructed using nichrome wire embedded in a ceramic. The construction at the condenser end is similar except that the heating element is replaced with a copper water jacket through which cooling water can be circulated. The adiabatic section is constructed from Teflon and the entire assembly is placed in a box made from Teflon, 12 mm thick, to provide insulation at the edges and the bottom.

The heat pipe assembly is placed in a glass bell jar 305 mm in diameter and 457 mm high. The bell jar allows the system to be evacuated and the working fluid, R-11, injected so that experiments can be conducted in an environment free of noncondensable gases. The rest of the system, which is illustrated in Fig. 2, consists of an aluminum base ported to allow for electrical and plumbing access, a vacuum pump, a constant temperature bath to provide cooling water to the condenser and an auxiliary heater to assist in the control of the pressure, particularly during start-up, in the bell jar.

In addition to the thermocouples already discussed and located as indicated in Fig. 1, the heat flux meters contain integrally mounted thermocouples and a differential thermocouple was installed to measure the temperature difference from inlet to outlet for the condenser cooling water. The system pressure was measured using a dial gauge. This pressure was in turn used to calculate the saturation temperature from the following relationship which is a curve fit to the saturation data due to Jacobsen, *et al.* [10].

$$T_{\text{sat}} = -17.2522 + 53.15294P_{\text{sat}} - 12.3986P_{\text{sat}}^2 \quad (1)$$

where pressure is in bars and temperature is in °C.

The experiment was initiated by evacuating the bell jar using a vacuum pump. The working fluid, R-11, was then injected into the bell jar until the pressure reached 1 atm. The system was then again evacuated to further reduce the noncondensable gases. This procedure resulted in a concentration of noncondensable gases of less than 0.01% (theoretical). After the

second evacuation, R-11 was again injected into the bell jar and the auxiliary heater turned on to raise the pressure to between 1 and 2 psi above the barometric pressure. All experiments were conducted at pressures above atmospheric to eliminate the possibility of noncondensable gases entering the system. When the pressure reached the desired level cooling fluid was pumped to the condenser. Once the adiabatic and evaporator sections were flooded with condensate the evaporator was started by turning on the power to the heater. The heat pipe was then brought to steady state operation by adjusting the power input to the evaporator heater and/or the temperature of the condenser coolant.

All reported temperatures and heat fluxes were measured directly. The temperature and heat flux measurements have an estimated accuracy of $\pm 0.5^\circ\text{C}$ and $\pm 1 \text{ W m}^{-2}$, respectively. The saturation temperature was determined indirectly from the measured vapor pressure in the system. The maximum barometric pressure change during an experiment was 0.005 bar which leads to a 0.15°C in the calculation of the saturation temperature. The pressure gauge was accurate to ± 0.014 bar which leads to $\pm 0.4^\circ\text{C}$ in the calculation of saturation temp. Experiments were repeated on different days. Heat fluxes were repeatable to within $\pm 10\%$.

HEAT PIPE MODEL

As indicated in the introduction, one of the goals was to examine evaporator performance, thus, it was important to establish the conditions for which the heat pipe would be evaporator limited as opposed to condenser or wick limited. A simple model for the wick was developed to assist in estimating the conditions for which this would be the case. For the experimental heat pipe, which has a very large vapor flow path, it is expected that the vapor phase pressure drop is negligible. Thus, the capillary pressure and the liquid phase pressure in the wick can be equated. Using Darcy's law the liquid phase pressure drop in the wick can be estimated

$$\Delta P_1 = \frac{\mu_1 L_c \dot{m}_1}{\rho_1 K K_r A} \quad (2)$$

In equation (2) the effective path length for the wick is taken to be the length of the adiabatic section plus one half of each of the condenser length and the evaporator length. The difference in capillary pressure along the length of the wick can be approximated as

$$\Delta P_c = 2\sigma_1 \left(\frac{\cos \phi_e}{r_e} - \frac{\cos \phi_c}{r_c} \right) \quad (3)$$

If it is assumed that the condenser is saturated so that $\cos \phi_c / r_c \approx 0$ then these results can be equated leading to an expression for the maximum mass flow rate that can be delivered by the wick:

$$\dot{m}_w = \frac{2\rho_1 \sigma_1 K K_r A}{\mu_1 L_c r_c} \quad (4)$$

The maximum possible heat transport can then be written

$$Q = \dot{m}_1 h_{fg} = \left(\frac{\rho_1 \sigma_1 h_{fg}}{\mu_1} \right) \left(\frac{K K_r A}{r_c} \frac{2}{L_c} \right) \quad (5)$$

The first group of parameters in equation (5) characterizes the working fluid and is known as the figure of merit. The second group characterizes the physical properties of the wick. In this case it has been assumed that the working fluid wets the wick material completely ($\cos \phi_e = 1$). For the experimental heat pipe the figure of merit is approximately 10^{10} W m^{-2} and the second group is estimated to be 10^{-7} m^2 (taking $K_r = 1.0$). Thus, the wick has the capability to deliver $Q \sim 1000 \text{ W}$ ($\sim 207\,000 \text{ W m}^{-2}$).

In order to completely understand the limitations of the experimental heat pipe, the condenser must also be considered. The heat flux at the condenser can be approximated as follows:

$$q_c = \frac{\dot{m}_1 h_{fg}}{A_c} = \frac{k_{\text{eff}} \Delta T_{\text{sub}}}{\delta} \quad (6)$$

where δ is the average liquid film thickness on the condenser neglecting capillary effects which result in a two-phase capillary fringe. The effective thermal conductivity, k_{eff} , of the wick is estimated using the geometric mean [11]. Combining equations (5) and (6) while approximating the flow area in the wick, A , as $\delta \cdot w$ results in

$$Q = \left(\frac{\rho_1 \sigma_1 h_{fg}}{\mu_1} \right) \left(\frac{2 K K_r}{r_c L_c} \right) \left(\frac{k_{\text{eff}} \Delta T_{\text{sub}} w}{q_c} \right) \quad (7)$$

As indicated previously the merit number is approximately 10^{10} . The second group is approximately 3×10^{-4} (taking $K_r = 1$). At steady state operation $Q/A_c \approx q_c$, therefore,

$$q \approx 2.7 \times 10^3 \Delta T_{\text{sub}}^{1/2} \quad (8)$$

for the 4.762 mm thick wick. For the 3.175 mm thick wick the constant in equation (8) becomes 2.2×10^3 . The effective thermal conductivities were taken to be 0.151 W m K^{-1} for the 4.762 mm wick and 0.165 W m K^{-1} for the 3.175 mm wick in computing the constant in equation (8).

RESULTS AND DISCUSSION

Four wick configurations were examined in this study. All were fabricated from copper foametal (Hogen Industries, Inc., Mentor, Ohio). Three wick configurations used a 4.762 mm thick wick and one used a 3.175 mm thick wick. The properties of the wick materials are listed in Table 1.

Figure 3 shows the heat flux vs excess temperature for a 4.762 mm thick wick. These results imply that boiling is initiated at an excess temperature less than 1°C . The heat flux increased with excess temperature up to an excess temperature of approximately 6°C . At this point an increase in the heat flux resulted in a decrease in the excess temperature. This phenomenon has been observed by previous investigators [12, 13]. The explanation is that initially nucleation begins on the solid copper surface and in the smaller pores of the wick. The surface temperature is relatively high during these early stages of the nucleation process. As soon as nucleation is initiated over the entire wick the surface temperature drops. This drop in temperature is referred to as the overshoot temperature. There is a local peak in the heat flux in the overshoot region. Beyond this point further increases in excess temperature resulted in a decrease in heat flux. This continued until the excess temperature reached approximately 25°C . We speculate that in this range of excess temperatures a transition is occurring that is similar to the transition from nucleate pool boiling to film boiling although less spectacular. At the peak heat flux it is presumed that the surface is still primarily in

Table 1. Properties of foametal wicks

	Thickness [mm]	No. of channels on evaporator	Porosity [%]	Permeability [m^2]	r_c [mm]	w [mm]
1.	4.762	0	95	5×10^{-9}	0.23	76.2
2.	4.762	7	95	5×10^{-9}	0.23	65.1
3.	4.762	15	95	5×10^{-9}	0.23	53.3
4.	3.175	15	94	3×10^{-9}	0.23	53.3

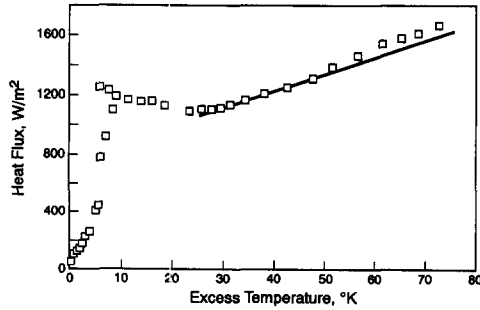


Fig. 3. Heat flux vs excess temperature for the 4.76 mm thick wick.

contact with liquid. However, beyond this point larger and larger portions of the surface are covered with a vapor film. At the minimum heat flux ($\Delta T \sim 25^\circ\text{C}$) the transition is complete resulting in a film boiling regime. In this regime the heat flux increase is approximately linear with excess temperature. Film thickness can be estimated from the experimental data by assuming heat transfer by conduction across a region where the foametal contains vapor only. The solid line shown in Fig. 3 is the calculated heat flux assuming a vapor film of the order of one pore diameter next to the evaporator surface. Experiments were run up to an excess temperature of approximately 80°C . The surface temperature remained uniform indicating that dry out was not experienced at the downstream end of the evaporator. Equation (8) estimates a performance limit of $\sim 10\,000\text{ W m}^{-2}$ at a typical $\Delta T_{\text{sub}} \sim 14^\circ\text{C}$. Thus, we conclude that for these experiments the heat pipe was evaporator limited.

For the next experiment, seven equally spaced channels 1.6 mm wide were cut in the wick at the evaporator end. The results are shown in Fig. 4. The maximum excess temperature, prior to overshoot, occurred at approximately 3.7°C . In this case the heat flux rose to above 2000 W m^{-2} at excess temperature below 5°C . This is a significant increase compared to the peak at approximately 1250 W m^{-2} for the surface without the channels. For this surface there was a less pronounced decrease in heat flux vs excess temperature in the transitional region. The linear increase in heat flux with excess temperature was again observed at large excess temperatures. For this surface hysteresis was examined as indicated in the figure. For

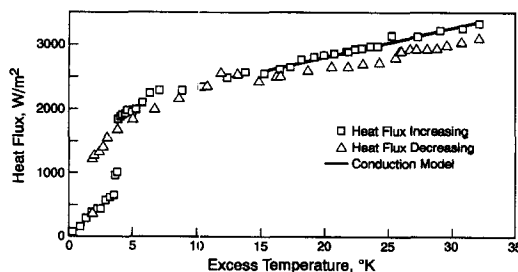


Fig. 4. Heat flux vs excess temperature for the 4.76 mm thick wick with seven channels.

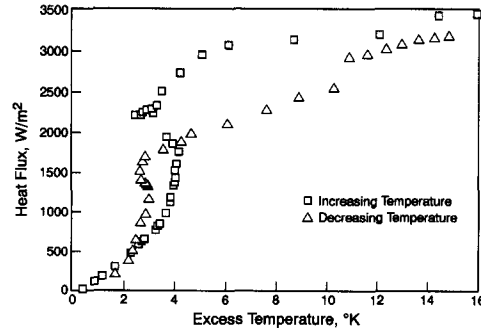


Fig. 5. Heat flux vs excess temperature for the 4.76 mm thick wick with 15 channels.

decreasing heat flux the heat flux was slightly lower at the same excess temperature. In addition, a minimum excess temperature of 2°C as opposed to 3.7°C was observed. All observations indicate that this wick also resulted in an evaporator limited heat pipe. For this case equation (8) yields a limit of approximately 4600 W m^{-2} at $\Delta T_{\text{sub}} \sim 4^\circ\text{C}$ (accounting for the fact that 85% of the surface is covered with the wick).

Figure 5 shows results for a 4.762 mm thick wick with 15 equally spaced channels 1.6 mm wide. In this case 70% of the evaporator surface is covered with the wick. Hence, the portion of the surface effective for boiling is considerably reduced but the vapor escape path offers considerably less resistance compared to a surface covered with a solid wick. The results are similar to those for the seven channel surface except that heat fluxes are typically higher at the same excess temperature. For this surface a heat flux of 2230 W m^{-2} was attained at an excess temperature of 2.5°C . A heat flux of 3500 W m^{-2} was observed at an excess temperature of 16°C . In the case of the seven channel surface an excess temperature of 35°C was necessary to achieve this same heat flux. The hysteresis was more pronounced for this surface. At maximum flux the measured temperatures on the evaporator surface differed by as much as 13°C from upstream to the downstream side indicating dry out of the wick. The maximum heat flux predicted at the wicking limit for this case was $\sim 3800\text{ W m}^{-2}$, which is within 8% of the actual operating condition. It is believed that the large hysteresis may be a result of the necessity to rewet the wick as the heat flux was decreased.

The performance of all three surfaces (for increasing heat flux) is shown in Fig. 6 for comparative purposes. It is clear from this figure that the channels have a significant effect on the evaporator performance. A nucleate boiling curve predicted using the Rohsenow correlation [14] is plotted on the figure for reference. In the overshoot region the channeled surfaces exhibit a much higher heat flux than that for nucleate pool boiling at the same value of excess temperature.

A final series of experiments was conducted on a 3.175 mm thick wick with 15 channels. In this case dryout was expected to occur since equation (8) predicts a maximum heat flux of 2700 W m^{-2}

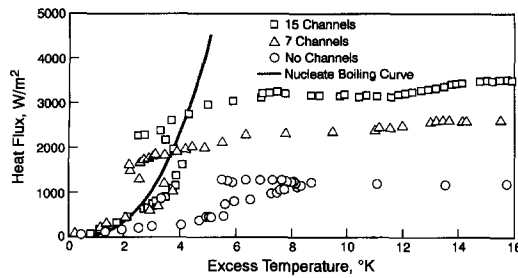


Fig. 6. Comparison of all of the results for the 4.76 mm thick wick.

($\Delta T_{\text{sub}} \sim 3^\circ\text{C}$ and 70% of surface wicked). This appears to be the case. A drop from the maximum heat flux which was in excess of 2600 W m^{-2} occurred as the excess temperature was increased beyond 20°C . This was accompanied by a considerable degree of hysteresis on the decreasing heat flux portion of the boiling curve. The dryout phenomenon can be further examined through the local temperature on the evaporator surface. These temperatures are plotted as a function of time in Fig. 8. Thermocouple locations are indicated in Fig. 1. The actual measured heat flux at several times is also indicated on the figure. At small values of the excess temperatures all three thermocouples read the same temperature. The thermocouple located farthest downstream (No. 7) began to deviate from the other two before the peak heat flux was reached. After the peak heat flux it increased very rapidly. Eventually the two upstream thermocouples exhibited a similar increase. The downstream thermocouple remained at a temperature significantly above the other two for an extended period during which the heat flux was being decreased. This indicated that it took considerable time for the wick to completely rewet. These observations are consistent with the statements made earlier with regard to hysteresis.

It is worth noting that R-11 is a poor choice of working fluid for this application. It was selected for these experiments because of its low saturation temperature and relatively low latent heat. However, the figure of merit for R-11 is in excess of three orders of magnitude less than that for water. This means that the wicking limit for R-11 is much smaller than water

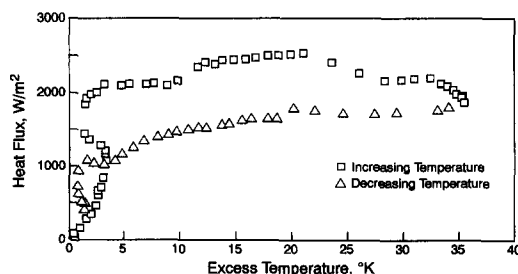


Fig. 7. Heat flux vs excess temperature for the 3.12 mm thick wick with 15 channels.

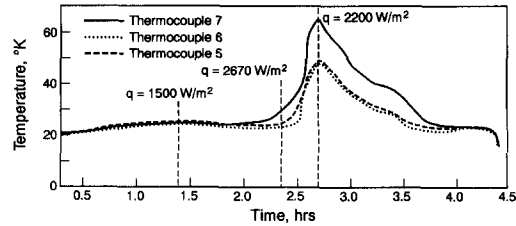


Fig. 8. Temperature vs time on the evaporator surface with the 3.12 mm thick wick and 15 channels.

and that water would rewet the wick much more rapidly.

CONCLUSIONS

The heat and mass transfer in a horizontal heat pipe, with emphasis on the evaporator, were studied experimentally. The working fluid for all experiments was R-11. The performance of porous metal wicks with and without channels cut in the evaporator section was examined. The particular heat pipe geometry studied was evaporator limited when a wick with no channels in the evaporator section was used. It is illustrated that the performance of the evaporator can be improved significantly by cutting channels in the wick. It is postulated that this is because the channels provide a low resistance path for the vapor to escape thus delaying the onset of a film boiling regime in which a vapor film blankets the evaporator surface.

Experiments were conducted with seven and 15 1.6 mm wide channels cut in a foametal wick covering an evaporator surface which was 63.5 mm long \times 76 mm wide. The evaporator performance, as measured by the heat flux above which the transition from nucleate to film boiling began, increased by as much as 125% for the surface with seven channels and 200% for the surface with 15 channels as compared to the surface with no channels.

The experimental parameters allowed the dryout conditions to be explored for some of the channeled wicks. These are the conditions for which the wicking limit is approached and the wick can no longer deliver sufficient liquid to all areas of the evaporator. In this case surface temperatures on the evaporator increase dramatically and the boiling curves which plot heat flux as a function of excess temperature show considerable hysteresis. This hysteresis appears to be a result of the rewetting process.

These results indicate that considerable improvement in heat pipe performance may be possible if the wick is carefully designed to provide optimum performance for all three functions: condensing, boiling and wicking.

REFERENCES

1. P. D. Dunn and D. A. Reay, *Heat Pipes* (3rd Edn). Pergamon Press, New York (1982).
2. C. K. Cheng and C. A. Lee, Heat transfer characteristics of a closed loop two phase thermosyphon system for

- solar collector applications, *Proceedings of the 5th International Heat Pipe Conference*, Japan Technology and Economics Center, Vol. 1, p. 301 (1985).
3. A. Abhat, High performance heat pipe for latent heat thermal energy storage applications, *Proceedings of the 5th International Heat Pipe Conference*, Japan Technology and Economics Center, Vol. 1, p. 321 (1985).
 4. P. J. Marto and G. P. Peterson, Application of heat pipes to electronic cooling. In *Advances in Thermal Modeling of Electronic Components and Systems* (Edited by A. Bar-Cohen and A. D. Kraus), pp. 283–336. Hemisphere, New York (1988).
 5. G. P. Peterson and P. F. Marshall, Analytical and experimental determination of heat pipe priming in micro-g. *Proceedings of the 5th International Heat Pipe Conference*, Vol. 1, pp. 434–438 (1984).
 6. Y. Cao and A. Faghri, Transient multidimensional analysis of nonconventional heat pipes with uniform and nonuniform heat distributions, *J. Heat Transfer* **113**, 995–1002 (1991).
 7. A. Shekarraz, and O. A. Plumb, Enhancement of film condensation using porous fins, *AIAA J. Thermophys. Heat Transfer* **3**(3), 309–314 (1989).
 8. B. G. Jones, J-Y Sun and C. Pan, Electronic cooling through porous layers with wick boiling, *Proceedings of the National Heat Transfer Conference* (Edited by H. R. Jacobs), Vol. 1, pp. 523–532 (1988).
 9. R. A. Moss and A. J. Kelley, Neutron radiographic study of limiting heat pipe performance, *Int. J. Heat Mass Transfer* **13**(3), 491–502 (1970).
 10. R. T. Jacobsen, E. W. Lemmon, S. G. Penoncello, S. W. Beyerlein and M. J. Ford, Personal computer programs for calculating thermodynamic properties from fundamental equations of state for fluids of engineering interest, Center for Applied Thermodynamic Studies, University of Idaho (1992).
 11. M. Kaviany, *Principles of Heat Transfer in Porous Media*, pp. 117–127. Springer, New York (1991).
 12. M. Z. Tongze, Zhengfrag and L. Huiquin, Vaporization heat transfer in capillary wick structure formed by sintered screens, *Proceedings of the 5th International Heat Pipe Conference*, Japan Technology and Economics Center, Vol. 1, p. 156 (1985).
 13. I. M. Honda, Oshiro, A. Suzuki, Y. Abe and S. Sugihara, Experimental study of a naphthalene heat pipe, *Proceedings of the 5th International Heat Pipe Conference*, Japan Technology and Economics Center, Vol. 2, p. 93 (1985).
 14. J. W. Westwater, J. C. Zinn and K. J. Brodbeck, Correlation of pool boiling curves for homologous group: freons, *J. Heat Transfer* **11**, 204–206 (1989).